

Component Distribution of Alcohol Ethylene Oxide Adducts

D. R. WEIMER and D. E. COOPER, Continental Oil Company, Ponca City, Oklahoma

Abstract

The relative reaction constants for the base-catalyzed ethoxylation of primary straight chain alcohols have been determined for the unreacted alcohol and the first three ethylene oxide adducts. The distribution of the ethoxylates was found using molecular distillation, nuclear magnetic resonance analysis and gas liquid partition chromatography.

A mathematical model describing the distributions was set up and programmed on a 7090 digital computer. Solution of the program gave the relative reaction constants for the alcohol and the first three adducts.

The relative reactivities of the adducts in the base-catalyzed ethoxylation of primary straight chain alcohols are shown to increase with adduct number, but tend to a constant value as the adduct number increases. Results also show that alcohols from C_6 to C_{18} are equally reactive to ethylene oxide on a molar basis.

Introduction

ETHYLENE OXIDE adducts (ethoxylates) of long chain alcohols have been commercially important for a number of years. The largest application for these ethoxylates is for nonionic detergents and ether sulfates. Although the ethoxylation reaction has been known for a number of years (5) the distribution of components in the product has been a controversial subject. In 1940 Flory postulated the theory that the product distribution obtained from the reaction of ethylene oxide with an active hydrogen compound followed the Poisson distribution (2). This theory was accepted until better analytical tools made the product distribution analysis possible. However, no simple analytical method has yet been devised where routine analysis can be made on the distribution of detergent range ethoxylates.

In recent years evidence has been given that the base-catalyzed ethoxylation of detergent range primary alcohols gave a Poisson distribution of components (6). Other evidence has been given that this reaction does not give a Poisson distribution of components (8,9). Probably the differences observed were due to the analysis of the products rather than any differences existing in the products. Our study deals only with the base-catalyzed ethoxylation of primary straight chain alcohols. Other alcohols and catalysts could give a different component distribution (9).

Process and Equipment

The ethoxylations for the study were done in pressure equipment and, in some cases, glassware. A diagram of the pressure equipment is given in Figure 1.

The alcohol and catalyst were charged to the autoclave through the liquid charge line. Air was purged from the system with nitrogen. The autoclave was then evacuated to remove the nitrogen. The alcohol and catalyst were heated to reaction temperature and ethylene oxide addition was started. The addition of the ethylene oxide was controlled by pressure demand through a research control valve equipped with a Foxboro Controller which was set at the desired reaction pressure. When the required amount of eth-

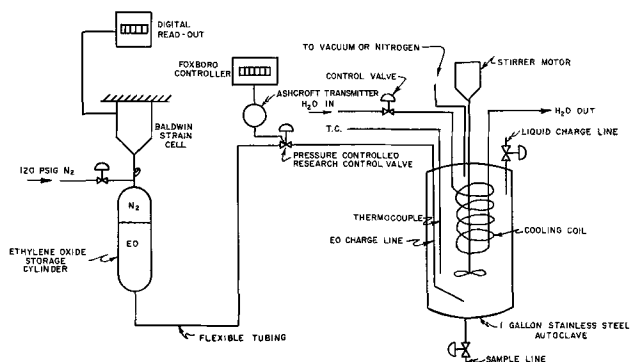


FIG. 1. Ethoxylation pressure equipment.

ylene oxide had been added, as measured by the weight loss of the ethylene oxide container suspended on the Baldwin strain cell, the addition was stopped. The digital read-out of the Baldwin strain cell gave readings to the nearest $2/1000$ of a pound. The reactor contents were post-stirred until essentially all of the ethylene oxide had reacted. The end of the reaction was determined by a drop in pressure to a constant level. The autoclave and reaction product were then cooled by running cold water through the cooling coils. In most cases the autoclave was under vacuum after cooling. The product was removed from the autoclave through the bottom sample line and weighed as a secondary check on the weight of ethylene oxide added. The product was neutralized with glacial acetic acid and stored for later analysis.

The glassware ethoxylations were done at slightly above atmospheric pressure maintained by a dip tube on the vent line submerged in a cylinder of mineral oil creating a hydrostatic head not exceeding 2.5 cm of mercury giving a pressure of approximately 0.48 psig.

Analysis of Product

Distillation of Ethoxylates

The unreacted alcohol and 1 mole adduct were removed by column distillation at reduced pressure. For the *n*-decanol (C_{10} alcohol) and *n*-dodecanol (C_{12} alcohol) ethoxylate products a 24 in. \times 1 in. column packed with $.16 \times .16$ in. stainless steel protruded packing was used. The heavier ethoxylate products were done on an 18 in. \times 1 in. column with the same type packing. The packing gave one theoretical plate per inch.

The bottoms from the distillation column were charged to a modified brush still. A head pressure of 1 to 20μ was maintained with a 200μ pressure drop occurring across the column. Cuts were taken during the distillation. In each distillation a point was reached where the pressure suddenly rose. This pressure rise was due to decomposition of the product. Toward the end of the distillation the pressure was closely watched and as soon as the pressure rose the distillation was stopped. The cuts from the distillation and the bottoms were analyzed by gas liquid chromatography (GLC) and nuclear magnetic resonance.

Gas-Liquid Chromatography

The analyses were done on a F & M Model 500 programmed temperature chromatograph. A 9 ft \times $1/4$

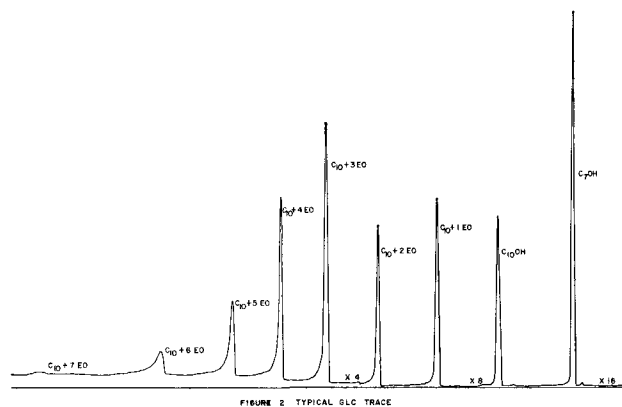


Fig. 2. Typical GLC trace.

in. copper column of 10% DYL T polyethylene packed on 80–100 mesh Gas-Chrom Z was used. Copper columns with other types of packing will give oxidation of alcohols to aldehydes, but this was not experienced with the above column.

The conditions for the analyses were: 130C starting temperature, 11C/min program rate, 65 ml/min helium flow and 305C maximum temperature.

Due to column holdup it was not possible to see all of the adducts in the samples. For example, with a C_{10} ethoxylate it was possible to see only as high as the 8th adduct (y_8). In order to compensate for column holdup and difference in thermal conductivity of the adducts, correction factors were determined to make the analyses quantitative. Pure alcohol ethoxylates which had been made from n-alkyl bromide and polyethylene glycols were mixed in various known proportions. To the adduct mixtures were added known amounts of the corresponding alcohol and n-heptanol (C_7 alcohol) as an internal standard. Analysis of the samples on the above column gave the required correction factors.

Changes in correction factors with changes in component concentrations were not significant. In order to check the effect of higher adducts on the correction factors for the alcohol and lower adducts, a sample of typical alcohol ethoxylate was analyzed using an n-heptanol (C_7 alcohol) internal standard and the correction factors. The weight per cents of the alcohol and lower adducts were calculated. Then a weighed amount of one of the lower adducts was added. Analysis of this sample using the C_7 alcohol internal standard and the correction factors gave an increase in the adduct peak corresponding to the amount of pure adduct added.

A GLPC trace of a typical C_{10} alcohol ethoxylate containing 40.8% ethylene oxide with 24.22 weight per cent C_7 alcohol added as an internal standard is given in Figure 2.

TABLE I

Gas Chromatography Analysis of a Typical C_{10} Alcohol Ethoxylate

	A	CF	B	W ₁	W ₂
C_7 OH	1014	1.000	1014	.242	
C_{10} OH	598	1.085	649	.156	.205
$C_{10} + 1$ EO	314	1.274	400	.096	.126
$C_{10} + 2$ EO	266	1.430	380	.091	.120
$C_{10} + 3$ EO	217	1.793	389	.093	.123

A = Area from GLC trace.

CF = Correction factors.

B = Corrected area.

W₁ = Weight fraction of total sample.W₂ = Weight fraction of ethoxylate sample.

C = Corrected total area.

A C_7 OH/W₁ C_7 OH = C.

A each component X CF = B each component.

B each component/C = W₁ each component.W₁/1.00 · W₁ C_7 OH = W₂.TABLE II
Comparison of GLC and NMR Analysis
of Ethoxylated n-Dodecanol

	Average moles EO/mole alcohol	
	NMR	GLC
Cut 1	0.00	0.00
2	0.32	0.29
3	0.79	0.77
4	1.05	0.99
5	1.77	1.67
6	2.54	2.38
7	2.88	2.75
8	3.51	3.34
9	4.46	4.14
10	5.35	4.89
Bottoms	9.14	

The peaks are identified on the trace as the C_7 alcohol, C_{10} alcohol and ethylene oxide adducts of the C_{10} alcohol.

The calculations to obtain the weight per cent of the lower adducts are similar to those used to obtain the correction factors. The method of the calculation of the trace in Figure 2 is shown in Table I.

The weight fraction of each higher adduct could not be calculated because no pure adducts were available to obtain the necessary correction factors.

Nuclear Magnetic Resonance Analysis

The method of NMR analysis has been previously described (1). The analyses on the cuts were given as the average moles of ethylene oxide per mole of alcohol. Primarily, the analyses were used as a check on GLC by comparing the values obtained from the two methods on the average moles of ethylene oxide per mole of alcohol.

A comparison of the two methods of analysis on the distillation cuts of n-dodecanol ethoxylated to 40 weight per cent ethylene oxide (2.82 moles) is given in Table II.

Analysis of the bottoms was not successful with GLC. The large increase in the NMR value from cut 10 to the bottoms was due to the large amount of bottoms from the distillation. Approximately one third of the distillation charge remained as bottoms.

Distillation of an n-decanol ethoxylated to 45.7% ethylene oxide gave better results, with the bottoms representing less than 10% of the distillation charge. Better correlation between GLC and NMR analyses was obtained on these cuts.

Reaction Variables

Before the data collected on the ethoxylates of different molecular weight alcohols were combined for the relative rate constant equations, the effect of molecular weight on the reactivity toward ethylene oxide was studied. This work was initially done using a blend of lower molecular weight alcohols. For example, a blend of C_6 , C_8 and C_{10} alcohols was used to facilitate the analyses. It was found that the alcohols are equally reactive to ethylene oxide on a molar basis. Figure 3 shows the per cent of each alcohol remaining at different ethylene oxide-alcohol ratios.

If the alcohols were not equally reactive the curve for each alcohol would be different. Such was not the case, as shown by the one curve for the alcohols.

This work was expanded to a blend of C_{12} , C_{14} , C_{16} and C_{18} alcohols. This blend gave similar results as with the C_6 , C_8 and C_{10} blend.

The reaction variables of temperature, pressure and catalyst were also studied. No significant differences were observed in the ranges: temperature, 180–220C; pressure, 0.48–80 psig; catalyst level, 0.125–0.3 weight

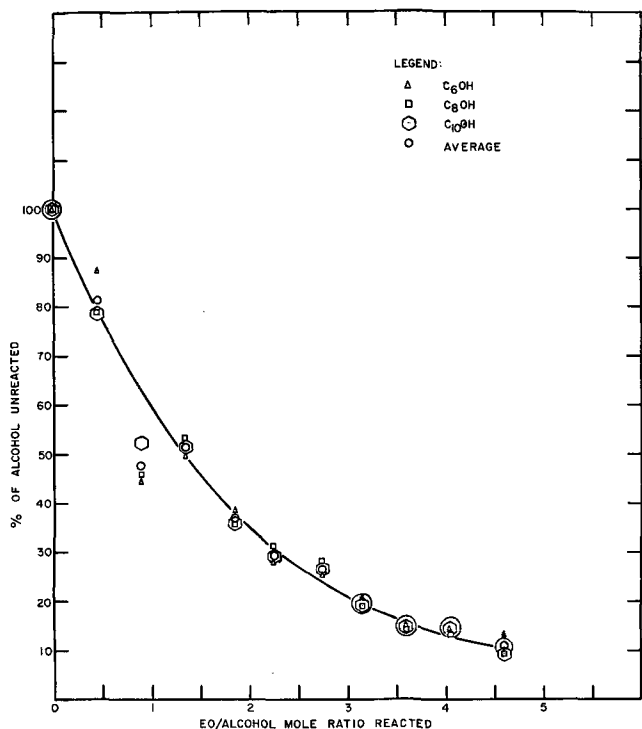


FIG. 3. Per cent unreacted alcohol in a blend.

per cent based on alcohol. Only the alkali metal hydroxides were used in the catalyst study. No significant difference in distribution was observed; however, the reaction rates are different. It should be pointed out that the data points plotted in Figures 4, 5, 6, 7 and 8 are from the ethoxylation of different molecular

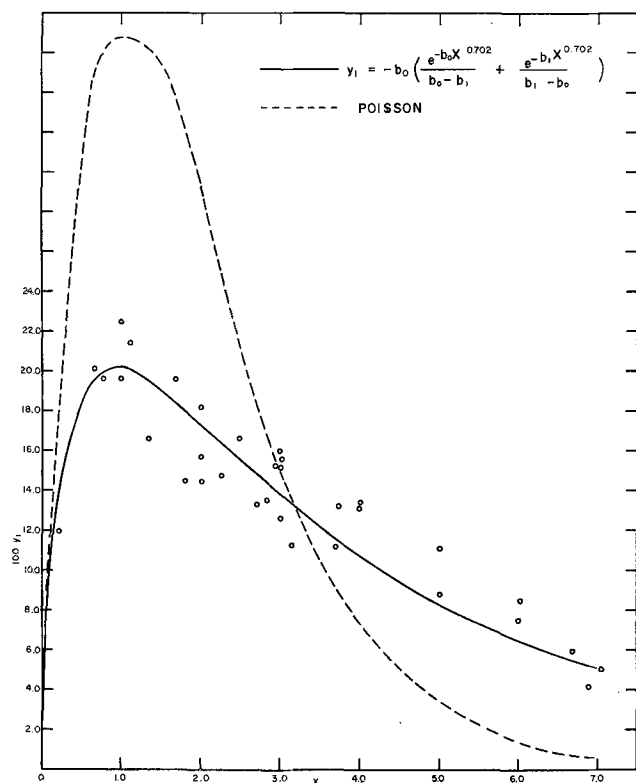


FIG. 5. Mole per cent of the first adduct as a function of ethylene oxide.

weight alcohols reacted at different pressures and temperatures.

Since no differences were observed in the above studies, the data on the different molecular weight alcohols were combined for the determination of relative rate constants.

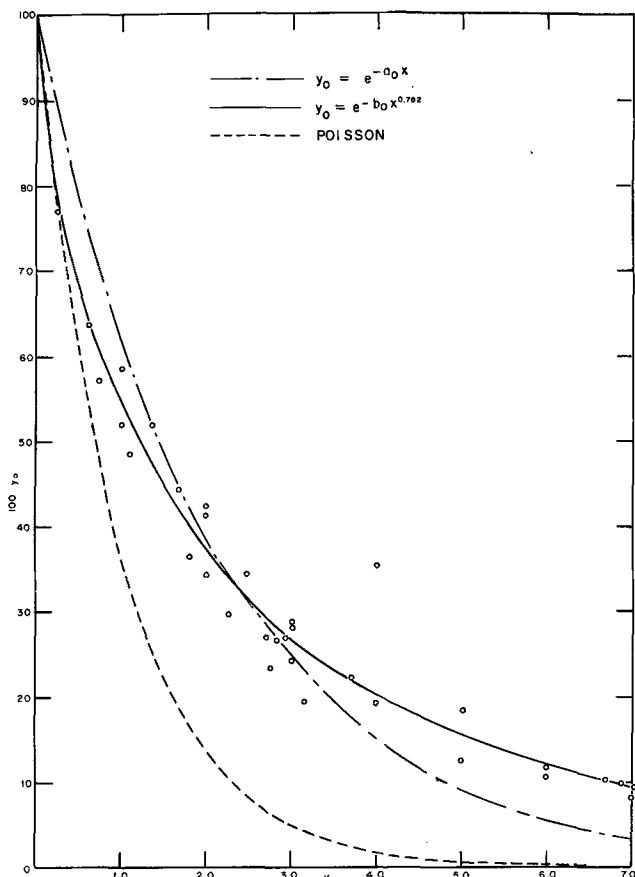


FIG. 4. Mole per cent of unreacted alcohol as a function of moles of ethylene oxide.

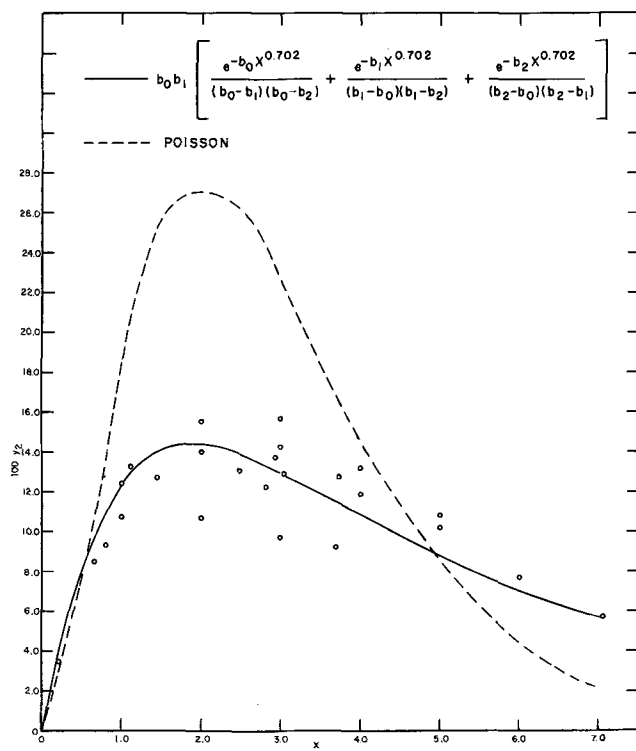


FIG. 6. Mole per cent of the second adduct as a function of ethylene oxide.

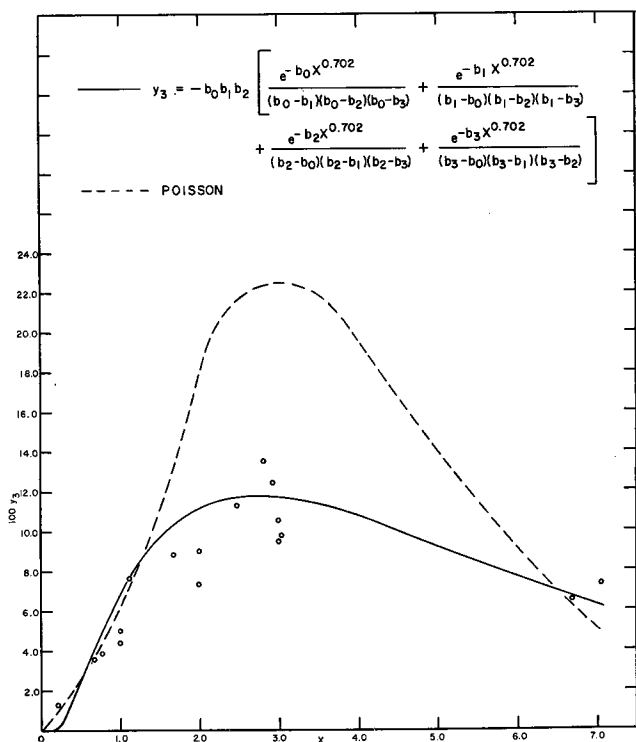


FIG. 7. Mole per cent of third adduct as a function of ethylene oxide.

Determination of Relative Rate Constants

Statistical techniques were used to derive a set of equations which would predict the distribution of adducts in the reaction product and hence the relative rate constants. Since the equations describing the reaction product are necessarily complicated, most of the previous work is based on assumptions which simplify the equations (2,10). However, the use of high speed computers makes it possible to determine con-

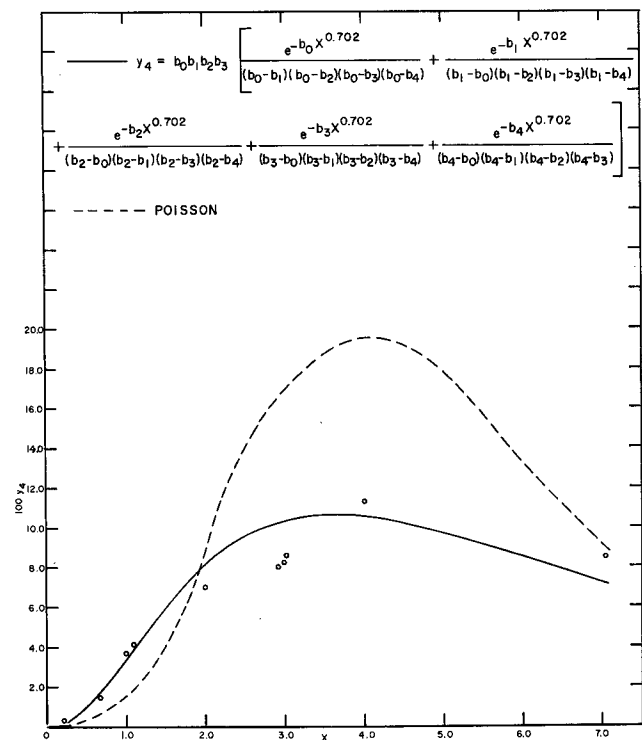


FIG. 8. Mole per cent of the fourth adduct as a function of ethylene oxide.

stants in complicated nonlinear equations and to evaluate alternative equations and select one which best fits the data.

The differential equations follow the approach proposed by Fuoss (3) and Weibull and Nycander (10).

The following notation is used:

- y_0 = mole fraction of unreacted alcohol in the reaction product
- y_i = mole fraction of the i th adduct in the reaction product
- x = number of moles of ethylene oxide per mole of alcohol
- a_i = relative rate constant for the i th adduct

As a first approximation the following differential equations were assumed:

$$\frac{dy_i}{dx} = -a_0 y_0 \tag{1}$$

$$\frac{dy_0}{dx} = a_{i-1} y_{i-1} - a_i y_i \quad (i = 1, 2, 3 \dots) \tag{2}$$

The solution to this system of equations can be written

$$y_0 = e^{-a_0 x} \tag{3}$$

$$y_i = \prod_{m=0}^{i-1} a_m \left[\sum_{\substack{j=0 \\ r \neq j}}^i \frac{e^{-a_j x}}{\prod_{r=0}^i (a_r - a_j)} \right] \quad (i = 1, 2, 3 \dots) \tag{4}$$

Equation (4) is equivalent to Weibull and Nycander's general equation (10) with y_0 replaced by $e^{-a_0 x}$.

In order to determine if equation (3) is a reasonable approximation for the unreacted alcohol, the data plotted in Figure 4, which includes results from the literature as well as results from the present study, were used to determine a_0 by least squares. The dash-dot curve plotted in Figure 4 represents the least squares fit to equation (3).

Although there is considerable scatter in the data, it is evident from Figure 4 that the simple exponential decay function $e^{-a_0 x}$, does not fit the data adequately, although it is considerably better than the Poisson. Since the data points tend to lie below the curve, $e^{-a_0 x}$, for low values of x and above the curve for high values of x , a power transformation on x is suggested.

If x is replaced by a transformed variable, $z = x^a$, equations corresponding to (1) and (2) can be written:

$$\frac{dy_0}{dz} = -b_0 y_0 \tag{5}$$

$$\frac{dy_i}{dz} = b_{i-1} y_{i-1} - b_i y_i \quad (i = 1, 2, 3 \dots) \tag{6}$$

where the b_i are rate constants relative to z .

The solutions corresponding to equations (3) and (4) in terms of the transformed variable are given by:

$$y_0 = e^{-b_0 z} = e^{-b_0 x^a} \tag{7}$$

$$y_i = \prod_{m=0}^{i-1} b_m \left[\sum_{j=0}^i \frac{e^{-b_j z}}{\prod_{\substack{r=0 \\ r \neq j}}^i (b_r - b_j)} \right] \quad (i = 1, 2, 3 \dots) \tag{8}$$

Example:

$$y_2 = b_0 b_1 \left[\frac{e^{-b_0 z}}{(b_1 - b_0)(b_2 - b_1)} + \frac{e^{-b_1 z}}{(b_0 - b_1)(b_2 - b_1)} + \frac{e^{-b_2 z}}{(b_0 - b_2)(b_1 - b_2)} \right]$$

Since the parameters a and b_i are nonlinear in equations (7) and (8), a nonlinear estimation technique is required to determine them from the data. A technique based on least squares is described by Hartley (4) and Peterson (7) which can be adapted to high speed computers. This technique employs a first order expansion around starting values of the parameters. This linearizes the equations and determines adjustments to be made on the parameters to improve the fit.

The process is iterated until a minimum is obtained for

$$\sum_{j=1}^{n_1} (y_{ij} - \hat{y}_{ij})^2 \quad (9)$$

where

y_{ij} = the j th observation on y_1

\hat{y}_{ij} = the j th value of y_1 computed from equations (7) and (8)

n_1 = number of observations on y_1

The exponent a in the transformation $z = x^a$ was determined from

$$\ln y_0 = -b_0 x^a \quad (10)$$

such that $\sum_{j=1}^{n_0} (\ln y_{0j} + b_0 x_j^a)^2$ is a minimum. An a value of 0.702 was obtained from the y_0 data. The solid line in Figure 4 illustrates the effectiveness of the power transformation.

The relative rate constants b_i were determined sequentially from the respective y_1 data; i.e., b_0 was determined from the data on y_0 . This b_0 was then used in the equation for y_1 to determine b_1 from the y_1 data, etc. At each stage of the nonlinear estimation procedure the b_i was determined such that equation (9) was minimized.

The relative rate constants, b_i , determined in this manner are shown in Table III for the first four adducts ($i = 0, 1, 2, 3, 4$). Table III also contains the constants for $a = 1.0$ and the estimated standard errors obtained from:

$$S_i = \sqrt{\frac{\sum_{j=1}^{n_1} (y_{ij} - \hat{y}_{ij})^2}{n_i - 1}}$$

The smaller standard errors for $a = 0.702$ is further evidence of the effectiveness of the power transformation.

TABLE III
Relative Distribution Constants (b_i & a_i)
for Various Adduct Numbers (i)

i	$a = 0.702$		$a = 1.0$	
	b_i	s_i	a_i	s_i
0	0.605	0.041	0.467	0.069
1	1.681	0.018	1.231	0.030
2	2.084	0.017	1.428	0.026
3	2.374	0.019	2.343	0.046
4	2.490	0.020		

a = exponent of the number of moles of ethylene oxide reacted
 i = adduct number.
 b_i, a_i = relative distribution constants.
 s_i = standard error.

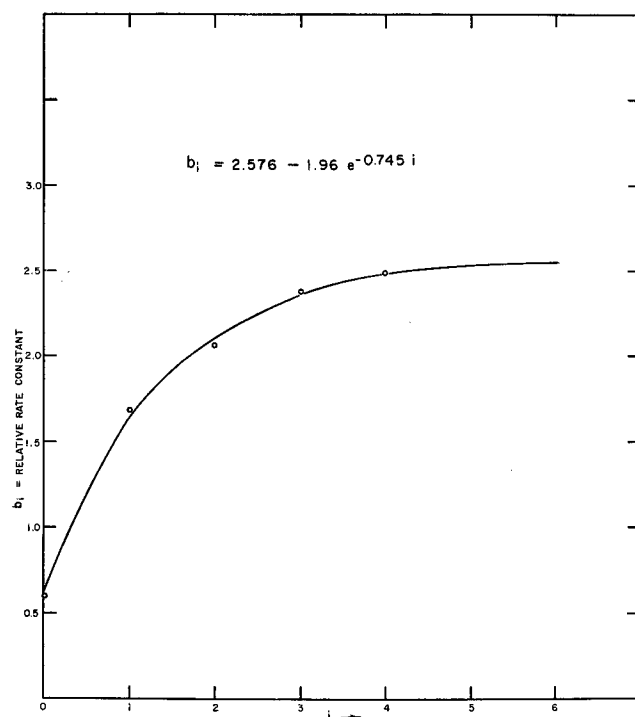


FIG. 9. Relative rate constants, b_i , as a function of adduct number, i .

Figures 5-8 show the observed points for the first four adducts with curves from equation (8) and the Poisson distribution. The equation for the specific y_1 is also shown in the figures. It is evident that the Poisson distribution is not adequate for this data.

The relative rate constants, b_i , are plotted in Figure 9 as a function of the adduct number. An equation of the form

$$\hat{b}_i = A + B e^{-C i} \quad (11)$$

proved to provide good prediction of the relative rate constants and allows estimates of the relative rate constants for the higher adducts through extrapolation. The parameters A , B , and C were determined such that

$$\sum_{i=0}^4 (b_i - \hat{b}_i)^2$$

is a minimum using the nonlinear estimation technique described previously. The resulting equation which generates the relative rate constants is

$$\hat{b}_i = 2.576 - 1.964 e^{-0.745 i} \quad (12)$$

The curve for equation (12) is shown in Figure 9. The form for this equation is in agreement with the theory that $b_i < b_{i+1}$ for the lower adducts and $b_i \rightarrow b_{i+1}$ where i is large.

TABLE IV
Mole Percent Individual Adducts (y_0 - y_8)
in C_{10} Alcohol + 3 Moles E.O.

	Theoretical	NMR	GLC
y_0	26.59		27.0
y_1	14.09	14.4	15.0
y_2	12.71	13.0	13.0
y_3	11.85	11.5	11.0
y_4	10.47	9.7	9.0
y_5	8.50	7.8	7.5
y_6	6.27	5.5	
y_7	4.20	4.5	
y_8	2.56	3.0	

TABLE V
 Theoretical Mole Percent Individual Adducts (y_0 - y_8) at Various Average Moles Ethylene Oxide (X) in Product

X	100 y_0	100 y_1	100 y_2	100 y_3	100 y_4	100 y_5	100 y_6	100 y_7	100 y_8	Sum. y_0 - y_8
0.5	68.62	19.14	7.89	3.00	0.99	0.28	0.07	0.01	0.00	100.00
1.0	54.19	20.71	12.27	6.94	3.48	1.53	0.59	0.20	0.06	99.97
2.0	36.92	17.88	14.15	11.24	8.23	5.41	3.18	1.68	0.80	99.44
3.0	26.59	14.09	12.71	11.85	10.47	8.50	6.27	4.20	2.56	97.24
4.0	19.77	10.97	10.59	10.83	10.71	9.92	8.48	6.67	4.79	92.73
5.0	15.02	8.52	8.59	9.29	9.90	10.03	9.50	8.34	6.78	85.97
6.0	11.59	6.70	6.90	7.75	8.67	9.36	9.56	9.14	8.16	77.83
7.0	9.06	5.29	5.53	6.36	7.38	8.34	9.00	9.20	8.83	68.99
8.0	7.16	4.20	4.44	5.19	6.17	7.22	8.13	8.75	8.91	60.17

The quantity

$$Q = \sum_{i=0}^4 \sum_{j=1}^{n_i} (y_{10} - \hat{y}_{10})^2$$

was computed using the b_i in Table III and compared with Q using \hat{b}_i from equation (12). The latter value was 0.0811, which compares favorably with $Q = 0.0766$ for the original b_i . Thus the relative rate constants obtained from equation (12) do not significantly increase the overall lack of fit.

Experimental verification of the extrapolated constants is given by comparing the theoretical distribution obtained using these constants with the distribution actually obtained on a sample of *n*-decanol ethoxylated to 3.0 moles of ethylene oxide. The analysis of the adducts was based on NMR analysis of the distillation cuts plotted: mole fraction of cuts in sequence vs. the average mole ratio of ethylene oxide per alcohol for the cut. The mole fraction of each adduct was then taken from the curve. Since this type of analysis is not valid at the extremes of the curve, the alcohol mole fraction and the mole fraction of the adducts higher than y_8 were not used. Also included is the GLC analysis of the cuts through y_5 . The data are given in Table IV.

Table V shows the theoretical distribution of reaction product through the eighth adduct, based on distribution constants from equation (12) and distribution equations (7) and (8). The corresponding curves are plotted in Figure 10 for adducts 5 through 8. Although equation (8) is quite complicated, especially for the higher adducts, the time required to compute the values in Table V on the 7090 computer was only 12 seconds. It should be pointed out that term by

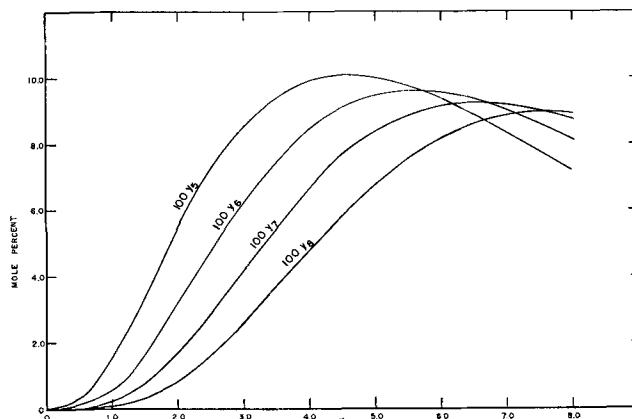


FIG. 10. Theoretical curves for mole per cent of y_5 through y_8 as a function of ethylene oxide.

term evaluation of equation (8) may lead to serious roundoff errors for $i > 5$ unless double precision arithmetic is used.

ACKNOWLEDGMENT

C. L. Hassell and J. D. Paden assisted in writing the computer programs; analytical assistance by A. B. Carel, J. W. Wimberley, P. W. F. Flanagan and C. E. Godsey.

REFERENCES

1. Flanagan, P. W., H. F. Smith and R. A. Greff, *Anal. Chem.* **35**, 1283 (1963).
2. Flory, P. J., *J. Am. Chem. Soc.* **62**, 1561 (1940).
3. Fuoss, R. M., *J. Am. Chem. Soc.* **65**, 2406 (1943).
4. Hartley, H. O., *Technometrics* **3**, 269 (1961).
5. I. G. Farbenindustrie, Brit. Patent 271,169 (Feb. 22, 1926).
6. Karabinos, J. V., and E. J. Quinn, *JAOCs* **33**, 223 (1956).
7. Peterson, T. I., *Chem. Eng. Prog., Symp. Ser.* **56**, 111 (1960).
8. Puthoff, M. E., and J. H. Benedict, *Anal. Chem.* **33**, 1884 (1961).
9. Stockburger, G. J., and J. D. Brandner, *JAOCs* **40**, 590 (1963).
10. Weibull, B., and B. Nycander, *Acta. Chem. Scand.* **8**, 847, (1954).

[Received January 28, 1966]